PROPERTIES OF LOW T_c SUPERCONDUCTING MULTILAYERS

Y. Bruynseraede, K. Temst, M. Baert, E. Rosseel, E. Osquiguil, V.V. Moshchalkov, C. Van Haesendonck
Laboratorium voor Vaste Stof-Fysika en Magnetisme, Katholieke Universiteit Leuven, B-3001 Leuven, Belgium

A. Gilabert
Laboratoire de Physique de la Matière Condensée, Université de Nice, F - 06034 Nice CEDEX, France

Ivan K. Schuller
Physics Department, University of California - San Diego, La Jolla, CA 92093-0319, USA

ABSTRACT: The properties of Pb/Ge and Al/Ge superconducting multilayers are reviewed. After a brief discussion of the preparation and structural characterization, a detailed analysis is presented of the superconducting interlayer coupling, the dimensionality effects and the anomalous critical current versus magnetic field behaviour in these multilayer structures.

INTRODUCTION

Artificially layered materials offer interesting opportunities to study physical phenomena on length scales of the order of the layering periodicity. A variety of new structural, electronic, magnetic, and superconducting properties have emerged and are currently the subject of intense experimental and theoretical efforts.[1] Since the advent of the high temperature superconductors (HTS), the interest in conventional superconducting multilayers has increased substantially.[2] Indeed, although there are important differences like the much shorter coherence lengths in HTS materials, the low T_c multilayers may act as model systems in which it is possible to vary at will the layer thicknesses, the interlayer coupling (proximity or Josephson) and hence the anisotropy, pinning strength, etc...

In this review article we will limit ourselves to a discussion of the well characterized Pb/Ge and Al/Ge multilayer structures.

PREPARATION:

The Pb/Ge and Al/Ge samples are prepared by electron beam evaporation in a MBE apparatus having a base pressure of 2×10^{-9} Torr. Typical evaporation rates, which are controlled by a quadrupole mass spectrometer, are 5 Å/s for Pb and Al and 1 Å/s for Ge. In order to obtain continuous thin Al and Pb films, the substrates (SiO_2 wafers) are held at liquid nitrogen temperature during the preparation. The low substrate temperature leads to crystalline Pb and Al layers, while the Ge is amorphous. The layer thicknesses are monitored with quartz crystal oscillators during the evaporation and calibrated with a Dektak surface profilometer. An independent cross-check for the calibration is obtained from X-ray diffraction spectra. The actual multilayer is produced by moving a shutter which alternately blocks one of the two material beams. Most samples consist of 5 or 10 bilayers with a thicker Ge protective capping layer on top.

The electrical transport measurements are performed on four terminal patterns (size 4.5×0.3 mm^2), which are obtained by combining electron beam lithography and lift-off. The low temperature measurements are carried out in a helium-4 cryostat equipped with a 15 T superconducting coil and in a helium-3 cryostat outfitted with a 7 T coil. In both systems the temperature can be varied with a stability of a few mK. The critical temperature T_c and the upper critical field H_{c2} are defined as the midpoint values of the recorded $R(T)$ and $R(H)$ transitions. Critical currents are obtained from both transport and magnetization experiments.

X-RAY DIFFRACTION:

X-Ray Diffraction is a technique that is well suited for the study of the superlattice structure. It is non-destructive and provides detailed information on both the superlattice quality (via the modula-

tion wavelength Λ) and the individual layer quality (via the lattice spacing d). Because only the diffracted X-ray intensity is measured in such an experiment, the phase information is lost. It is therefore impossible to convert the measured intensities directly into the structure of the crystal. Modeling of the superlattice is required to compare the calculated with the measured intensity. During the last few years the used structure models have evolved from the simple "step model" towards more sophisticated refinement procedures which allow a quantitative determination of the structure. For a systematic analysis of the experimental X-ray spectra a general kinematic formalism was developed which makes the application of numerical methods computationally feasible.[3] The model takes into account discrete and continuous thickness fluctuations of the layers, intralayer disorder and lattice strain near the interface. The non-linear Marquardt algorithm is used to refine peak positions, relative intensities, and line profiles. It is worth noting that the method is different from the well known Rietveld refinement procedure: in our refinement the relative intensities *and* the line profiles are used to determine the average unit cell and the statistical deviations from this average, whereas in Rietveld refinement the structure of a single unit cell is modeled and the relative intensity of the diffraction peaks is determined from the structure factor of the unit cell. The application of the refinement method to a variety of situations shows that the procedure gives reliable results for the cases for which the answer is known from independent measurements such as EXAFS, XPD, profilometry etc... The analysis of our experimental spectra for Pb/Ge multilayers will illustrate the strength of the refinement program. All spectra were obtained from θ - 2θ experiments using a Rigaku DII Max goniometer equipped with a rotating anode and capable of delivering a maximum power output of 12 kW. A laser system is used to secure an optimal alignment of the sample with respect to the X-ray beam. Data were taken using Cu K_α radiation with a wavelength $\lambda = 1.542$ Å. The diffracted radiation was filtered with a flat pyrolytic monochromator.

In Fig. 1 the measured X-ray diffraction spectra are shown for a Pb(46 Å)/Ge(29 Å) multilayer consisting of 5 bilayers. The low-angle spectrum
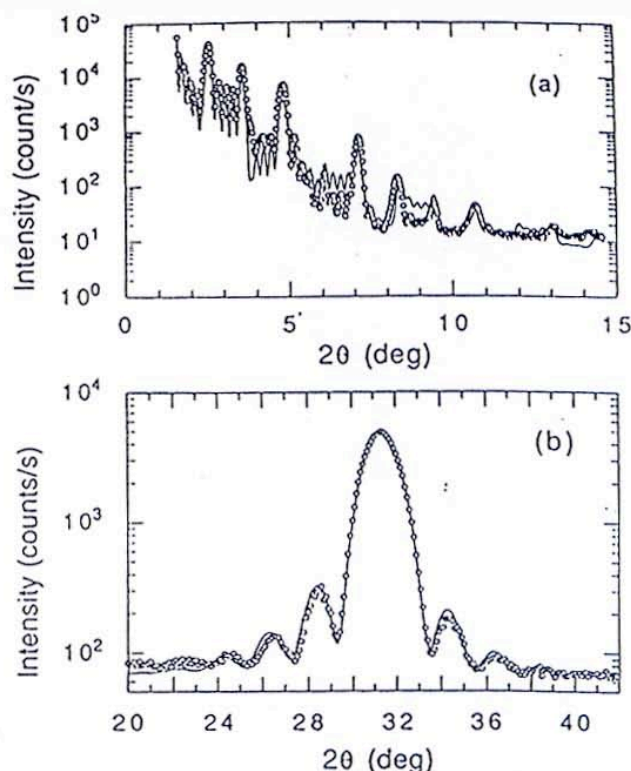

Fig. 1. Low (a) and high (b) angle profile of a [Pb(46 Å)/Ge(29 Å)]₅ multilayer. Open circles are the measured intensity and the solid line is the refined profile.

(Fig. 1 (a)) clearly shows a number of diffraction peaks, which can be attributed to the artificial layering. Using a modified Bragg law, the modulation length Λ can be calculated from the distance between the superlattice peaks. The peaks in between the superlattice reflections are due to the finite size effect. The full line in this graph is calculated using a recursive optical theory (which is exactly valid at low angles because it takes reflection of the X-ray beam into account) and assuming 1 Å of roughness on both layers. There is excellent agreement between the measured and calculated profile in both relative intensity and peak width. Fig. 1 (b) shows the high angle diffraction spectrum of the same sample together with the best fit calculated with the refinement program. Since the Ge layers are amorphous (i.e. we have to deal with a continuous roughness σ on the Ge), the observed pattern is typical for the diffraction spectrum from a single finite thickness crystalline Pb layer: a central peak corresponding to the Pb (111) reflection and a number of finite size peaks. It can be shown that for $\sigma=1.0$ Å , all traces of superlattice peaks disappear and the high angle

profile is solely produced by the finite size profile of a single crystalline layer, indicating that all crystalline Pb layers are decoupled and scatter incoherently.

In order to fit the width of the peaks it is necessary to introduce a discrete roughness on the crystalline Pb layers, i.e. a discrete Gaussian spread on the number of atomic planes within one crystalline layer. The introduction of discrete roughness on the crystalline component causes a decrease in the number of finite size peaks in the high angle region. Both discrete and continuous roughness broaden the lineshapes.

In order to obtain a still better agreement between the experimental and calculated spectra, the inclusion of intra-layer disorder is required, i.e. a small spread δ (with $\delta \ll d_{Pb}$) on the bulk Pb lattice distance. The asymmetry in the finite size peak intensities is explained by a slight lattice expansion Δd_{Pb} near the interface. The refined values yielded a Pb lattice spacing $d_{Pb}=2.846$ Å , a lattice expansion $\Delta d_{Pb}=0.03$ Å , and a discrete disorder of one monolayer ($\simeq 3$ Å). A number of other Pb/Ge samples were analysed in the same way and it was found that they were consistently best fit by including an intra-layer disorder δ of 0.04 to 0.06 Å . This intra-layer disorder is probably due to the low substrate temperature (77 K) during deposition, which is needed to grow continuous thin (< 250 Å) Pb films. The low temperature may inhibit the atomic mobility and the formation of a well defined crystalline structure.

SUPERCONDUCTING PROPERTIES

a) Critical fields:

The preparation of layered superconductor/normal metal or superconductor/insulator structures introduces an artificial anisotropy in their superconducting properties. Significant changes in the superconducting behaviour are therefore expected when the layer thicknesses are of the same magnitude as the superconducting coherence length $\xi(T)$. The anisotropy of $\xi(T)$ can be deduced experimentally from the upper critical field H_{c2}. In particular, the dimensional crossover in the temperature dependence of the parallel critical field $H_{c2}^{\parallel}$ was theoretically predicted and experimentally observed in a number of multilayers.[1]

The Ginzburg-Landau theory (valid in the vicinity of the critical temperature T_c) provides the following expressions for the upper critical fields parallel and perpendicular to the layers of a three dimensional (3D) anisotropic superconductor:

$$H_{c2}^{\parallel} = \frac{\Phi_0}{2\pi\xi_{\parallel}(T)\xi_{\perp}(T)} \qquad (1)$$

and

$$H_{c2}^{\perp} = \frac{\Phi_0}{2\pi\xi_{\parallel}^2(T)} \qquad (2)$$

Here Φ_0 is the superconducting flux quantum, $\xi_{\parallel}$ and $\xi_{\perp}$ are the superconducting coherence length parallel and perpendicular to the layered structure. The coherence length diverges near the critical temperature T_c as $(T_c-T)^{-1/2}$, leading to a linear temperature dependence for both $H_{c2}^{\parallel}$ and $H_{c2}^{\perp}$ for the 3D case.

If coupling between the superconducting layers is absent, the measured critical field is that of a stack of independent superconducting slabs. If these individual slabs are sufficiently thin, i.e. when the film thickness $d_s < \xi(T=0)$ they will behave as quasi-two dimensional (2D). The 'intrinsic' unperturbed coherence length ξ corresponds in a multilayer to the coherence length $\xi_{\parallel}$ in the plane of the superconducting layer. When $d_s \ll \xi_{\parallel}$ the parallel critical field is given by

$$H_{c2}^{\parallel} = \frac{\Phi_0\sqrt{12}}{2\pi\xi_{\parallel}(T)d_s} \qquad (3)$$

leading to a square root dependence of $H_{c2}^{\parallel}(T)$ in 2D.

In superconducting multilayers, the perpendicular coherence length $\xi_{\perp}$ is an important quantity because it reflects the extent of the superconducting coupling. For a well chosen thickness of the separator layer, the sample may change from an uncoupled to a coupled system as $\xi_{\perp}$ increases with increasing temperature. When $\xi_{\perp}(T)$ is of the same magnitude as the separator thickness d_{Ge}, superconducting coupling between the layers is established. This transition is usually referred to as the 2D - 3D dimensional crossover and has been observed in a variety of multilayered systems.[2)4)5)] Experimentally this transition can be observed by measuring $H_{c2}^{\parallel}(T)$ as shown in Fig. 2 for three different Pb/Ge multilayers. When the separator thickness $d_{Ge} > 30$ Å , the temperature dependence of $H_{c2}^{\parallel}$ follows a square root behaviour at all temperatures (Fig. 2a)). This indicates that there is no coupling between the layers and that

each layer is quasi 2D in nature. A dimensional crossover occurs when the Ge thickness $d_{Ge} \simeq 20$ Å (Fig. 2b)). Near T_c (where $\xi_\perp$ is large) the linear temperature dependence of $H_{c2}^\parallel$ is due to the coupling between the Pb layers. As the temperature is lowered, $\xi_\perp$ is reduced. When $\xi_\perp < d_{Ge}$ the magnetic flux is confined to the Ge layers, effec-
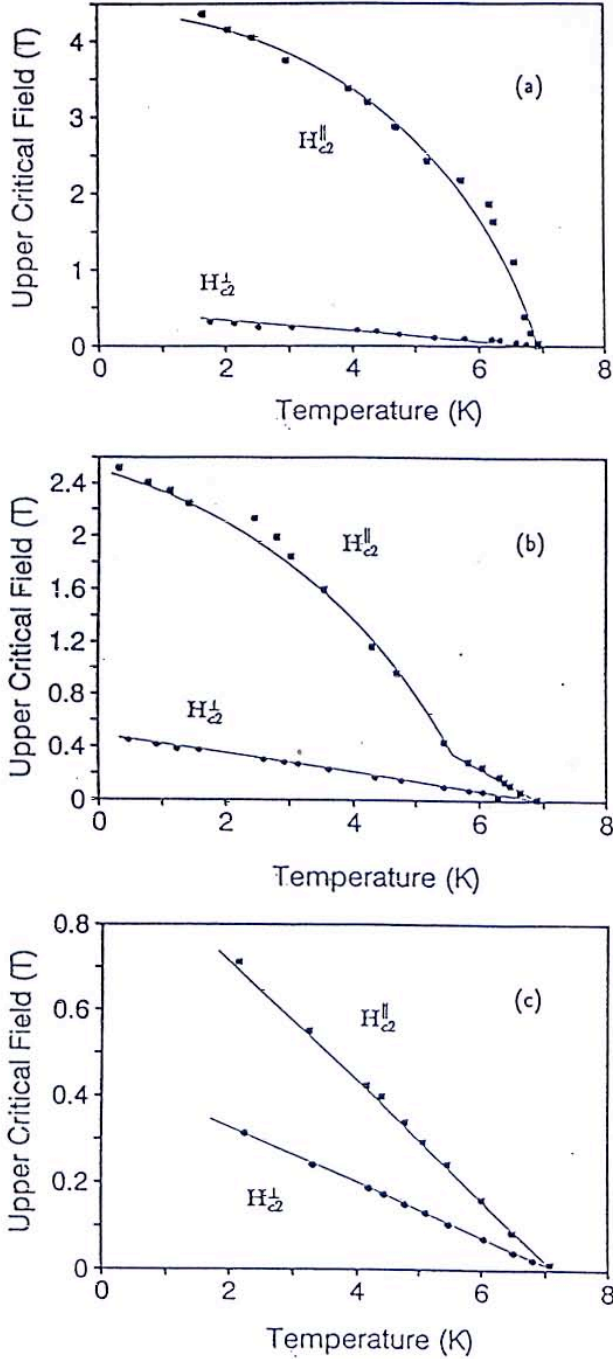
tively decoupling the 2D superconducting slabs. At this point a pronounced upturn in the temperature dependence of $H_{c2}^\parallel$ occurs. For a still smaller separator thickness, $d_{Ge}=15$ Å, a coupled 3D behaviour is observed (Fig. 2c)), producing a linear temperature dependence of $H_{c2}^\parallel(T)$.

Fig. 2 also shows the perpendicular critical fields of these samples. In all cases we observe a linear behaviour. This is due to the fact that the perpendicular critical field only probes the parallel coherence length $\xi_\parallel$, whereas the dimensionality of the system is given by $\xi_\perp$. Extrapolation of $H_{c2}^\perp$ towards low temperatures enables to derive a value for $\xi_\parallel(T \to 0) \simeq 280$ Å which is larger than the Pb layer thickness $d_{Pb}=140$ Å and justifies the treatment of each Pb layer as a 2D slab.

The coupling between superconducting layers has been analyzed theoretically by Klemm et al.[6] who treated the multilayer as a stack of 2D superconducting layers which are weakly coupled via *Josephson tunneling*. For *proximity coupled* systems $H_{c2}^\parallel(T)$ has been calculated by Takahashi and Tachiki[7] and Koyama et al.[8] The important parameters in this calculation are the ratio of the density of states, of the electronic diffusion coefficients, and of the BCS interaction constants of the normal and superconducting layer, respectively. These authors assume that the three parameters are constant within one layer and change discontinuously at the interfaces. This theory was successfully used to explain the dimensional crossover in Nb/Cu samples.[9] In order to explain the dimensional crossover in Pb/Ge samples with $d_{Ge} < 30$ Å, the ratio of the density of states $N_{Ge}/N_{Pb} \simeq 0.05$. This finite value for the density of states in Ge may be due to the existence of defect states within the bandgap near the Ge/Pb interface.

b) Superconducting fluctuations:

The dimensionality of a superconducting system can also be investigated by measuring the excess conductivity above T_c.[10] The amplitude and temperature dependence of the fluctuation conductivity provide detailed information on the dimensionality of the superconducting structures.

Aslamazov and Larkin[11] calculated the excess conductivity σ_{fl} for 3D systems in the Ginzburg-Landau approximation :

$$\sigma_{fl}^{3D} = \frac{e^2}{32\hbar\xi_0}\epsilon^{-1/2} \qquad (4)$$
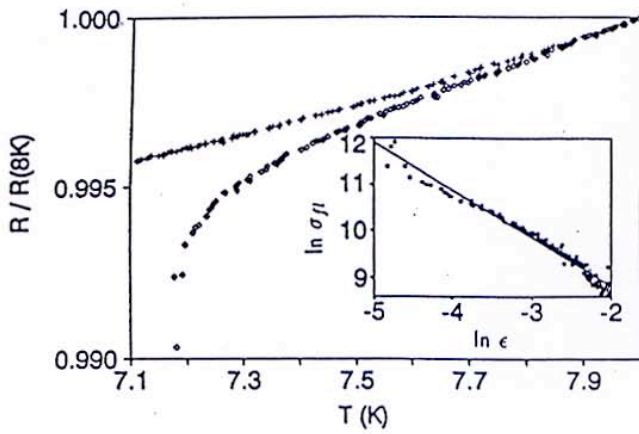
with $\epsilon = (T/T_c - 1)$.

Fig. 2. Parallel (■) and perpendicular (●) critical fields for Pb/Ge multilayers with $d_{Pb}=140$ Å and $d_{Ge}= 42$ Å (a), $d_{Ge}= 20$ Å (b) and $d_{Ge}= 15$ Å (c).

Fig. 3. *Zero field resistive transition of a [Pb(220 Å)/Ge(50 Å)]₁₀ multilayer (◇) compared to the normal state resistance (+). The inset shows ln σ_fl vs. ln (T/T_c-1).*

An analogous calculation for a 2D film with thickness d yields

$$\sigma_{fl}^{2D} = \frac{e^2}{16\hbar d}\epsilon^{-1} \qquad (5)$$

Fig. 3 shows the normalized zero field resistive transition of a Pb(220 Å)/Ge(50 Å) multilayer compared to the normal state resistance variation with temperature. This normal resistance is obtained by measuring the sample in a 1 T perpendicular field, which is higher than $H_{c2}^{\perp}(T\to 0)$. The presence of an important excess conductivity in zero field above T_c is a clear indication of the 2D nature of this multilayer. Plotting ln σ_{fl} as a function of ln ϵ (see inset Fig. 3) yields a slope equal to -1, which is in agreement with the 2D theoretical result (Eq. 5). Quantitative analysis showed the additional Maki - Thompson correction term to be negligible, due to the strong pair breaking in Pb.

By decreasing the Ge layer thickness from 50 Å to 25 Å, interesting dimensional crossover features can be observed in the excess conductivity. Fig. 4 compares the normal state resistance (again measured in a 1 T perpendicular field) with the resistive transitions measured in two different parallel magnetic fields. For $H_{||}$=0.07 T the sample is in the 3D part of the H - T phase diagram, while for $H_{||}$= 0.8 T the transition point shifts to the 2D part. In the latter case the resistive transition becomes obviously more rounded, characteristic for the appearance of 2D fluctuations. A more quantitative analysis confirms this change of dimensionality: the inset of Fig. 4 compares ln σ_{fl} versus ln ϵ for the two applied fields. The change of slope
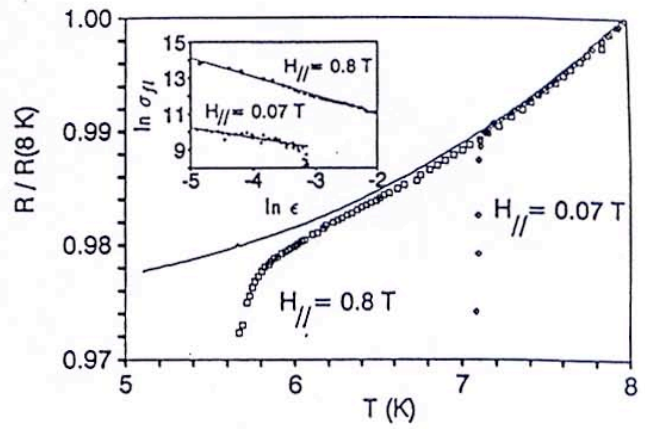

Fig. 4. *Resistive transitions of a [Pb(220 Å)/Ge(25 Å)]₁₀ multilayer in the 3D region (with $H_{||}$=0.07 T (◇)), and in the 2D region (with $H_{||}$=0.8 T (□)), compared to the normal state resistance (solid line). The inset shows ln σ_fl vs. ln (T/T_c-1) in both cases.*

from about -1/2 to -1 when a larger magnetic field is applied points to the change of dimensionality, thus confirming the results of the parallel critical fields measurements.

c) The anomalous Tachiki - Takahashi effect

The Pb/Ge system is very well suited to check other predictions of the Tachiki - Takahashi theory, in particular the behaviour of $H_{c2}^{||}(T)$ for different values of the ratio D_N/D_S, i.e. the ratio of the electronic diffusion constants. For a multilayer built from layers having the same density of states near the Fermi surface, equal BCS interaction constants, but different diffusion constants, the theory predicts an anomalous effect in the temperature dependence of the parallel upper critical field.[12] In order to meet the mentioned theoretical requirements we need two materials with the same critical temperature T_c but a different elastic mean free path. Therefore, Pb/Pb$_\alpha$Ge$_{1-\alpha}$ multilayers were prepared on liquid nitrogen cooled SiO₂ substrates, and consisting of 10 bilayers with 400 Å Pb and 400 Å Pb$_\alpha$Ge$_{1-\alpha}$ covered with a 200 Å protective Ge layer. The Pb$_\alpha$Ge$_{1-\alpha}$ layer was prepared by coevaporation of Pb and Ge. Using RBS measurements the relative concentration of Pb and Ge is determined to be close to 50 %. Both types of layers have a T_c=6.92 K, but the Ge inclusions in the Pb$_\alpha$Ge$_{1-\alpha}$ layer increase the resistivity compared to a pure Pb layer. As shown in Fig. 5, the $H_{c2}^{||}(T)$ for this multilayer has the well-known 3D - 2D crossover at T $\simeq$ 6.7 K. At
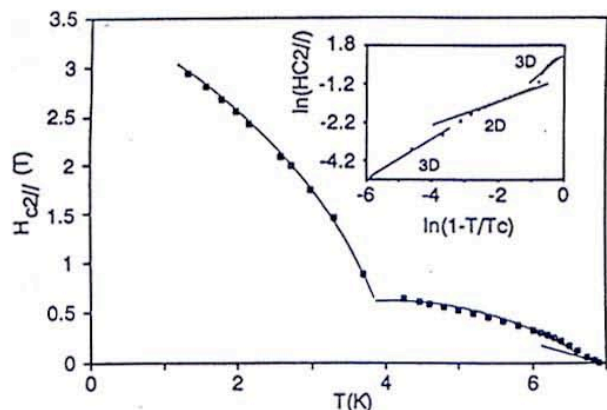
Fig. 5. $H_{c2}^{\parallel}(T)$ for a [Pb(400 Å)/PbGe(400 Å)]$_{10}$ multilayer. The inset shows $\ln(H_{c2}^{\parallel})$ vs. $\ln(1-T/T_c)$.

lower temperatures a marked upturn in the critical field is, however, observed. This sudden change of the slope in the H_{c2} curve can be explained as follows. Close to T_c the coherence length is large and therefore the superconducting order parameter averages over all layers, leading to a 3D linear $H_{c2}^{\parallel}(T)$ behaviour. As the temperature is lowered, ξ will decrease and nucleation of the order parameter will occur in either the clean (large diffusion constant D_N) Pb layers or in the dirty (small diffusion constant D_S) PbGe layers. Assuming that nucleation occurs in the Pb layers, only a small fraction of the order parameter will "leak" into the PbGe layers, because the latter's diffusion constant is small. Then the order parameter will be limited to the Pb layers and we observe indeed the typical 2D behaviour. The $H_{c2}^{\parallel}(T)$ behaviour is different for a clean and a dirty layer such that for still lower temperatures the critical field of the dirty PbGe layers exceeds that of the clean Pb layers. The coherence length is then much smaller than the PbGe layer thickness, leading again to a 3D behaviour. The sudden upturn in the critical field therefore corresponds to a shift in the nucleation position from the clean to the dirty layers and the H-T diagram shows a 3D - 2D - 3D transition. This is clear from the inset of Fig. 5 where $\ln(H_{c2}^{\parallel})$ is plotted versus $\ln(1-T/T_c)$. A fit to the data yields a slope 0.97 at high temperatures (3D), a slope 0.61 at intermediate temperatures (2D), and finally a slope 1.1 (3D) at the lowest temperatures.

d) Critical currents

Many of the theoretical ideas related to the ex-

istence of the irreversibility line in the H - T diagram of high T_c superconductors are based on the layered nature of these oxide materials and describe the flux line lattice as a superposition of two - dimensional pancake vortices.[13] In order to gain more insight into the behaviour of the flux line lattice in layered systems, it is very instructive to study the properties of the flux line lattice in artificially layered low T_c superconductors. We have performed a detailed study of the behaviour of the critical current when the field is applied perpendicular to the layers.[14] We observe that J_c drops to a minimum, followed by a broad maximum before finally decaying monotonously to zero with increasing magnetic field.
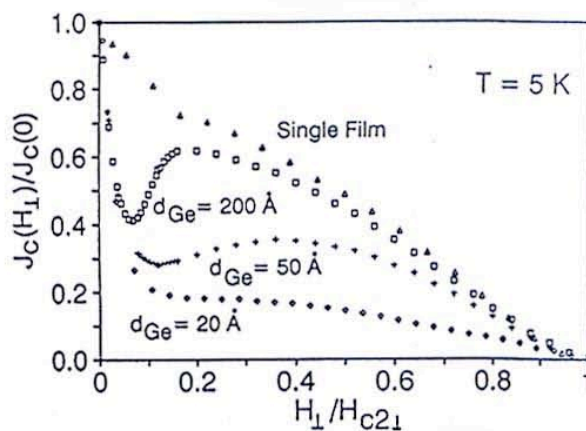

Fig. 6. Normalized critical current densities versus $H_\perp/H_{c2}^\perp$ for a single Pb film and for three Pb/Ge multilayers with $d_{Pb} = 200$ Å but different d_{Ge}.

The effect is dependent on the Ge layer thickness as is shown in Fig. 6 for a single Pb film (thickness 250 Å) and three multilayers with 50 bilayers of 200 Å Pb but varying Ge thickness. Here, the critical current was obtained from magnetization experiments. Because of uncertainties in the sample volume and the demagnetization factor, the data are normalized to their zero field value. The J_c of the multilayer with $d_{Ge}= 20$ Å Ge drops much faster than that of the single Pb film. For the multilayers with $d_{Ge}= 50$ Å and $d_{Ge}= 200$ Å, a clear minimum at H_1^* is observed in the J_c vs $H_\perp$ behaviour. The value of H_1^* is a function of d_{Ge} and of the temperature as shown in Fig. 7 where the minimum is not present anymore at T=1.4 K. The presence of the minimum is not limited to the Pb/Ge system as can be seen in Fig. 8 where $J_c(H_\perp)$ is shown for an [Al(220 Å)/Ge(220Å)]$_5$
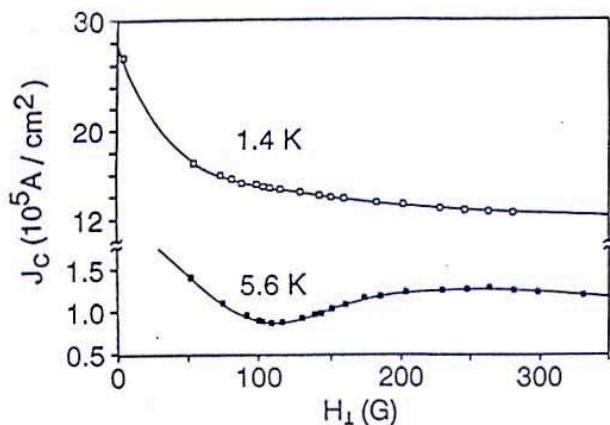
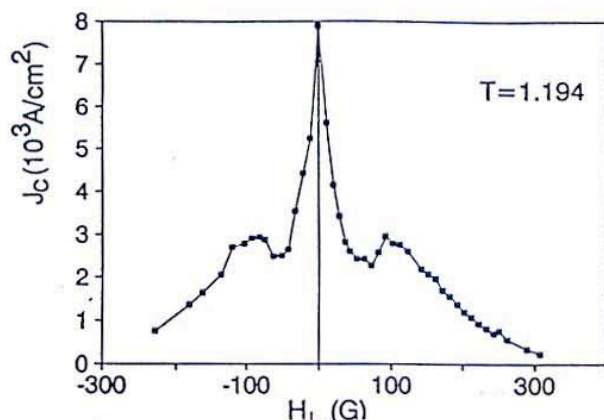Fig. 7. $J_c(H_\perp)$ for a $[Pb(140\ \text{Å})/Ge(50\ \text{Å})]_{10}$ multilayer at $T=6.5$ K and $T=1.4$ K.

Fig. 8. $J_c(H_\perp)$ for an $[Al(220\ \text{Å})/Ge(220\ \text{Å})]_5$ multilayer with $T_c = 1.68$ K.

Fig. 9. Schematic illustration of the $J_c(H_\perp)$ behaviour in a Pb/Ge multilayer according to the magnetic decoupling model.

multilayer in which the critical current densities are almost two orders of magnitude lower than in the Pb/Ge system. In Al/Ge we again observed the strong dependence of $H_\perp^*$ on d_{Ge}.

The minimum at $H_\perp^*$ can be interpreted as a softening of the flux line lattice, which might be explained in the framework of two theoretical models. The first is the melting of the initially 3D vortex lattice, which is due to the exponential decay of the vortex - vortex interaction at low fields such that the flux lattice is very sensitive to thermal fluctuations.[15] When pinning can be neglected, this causes the presence of a field regime above $H_{c1}^\perp$ where J_c should be zero, while J_c increases again at higher fields. If the pinning is strong enough, this melting transition will be suppressed. It can therefore be expected that for intermediate pinning strengths J_c should develop a minimum instead of dropping completely to zero. At low temperatures the thermal energy is insufficient to decouple the flux line lattice and the minimum is
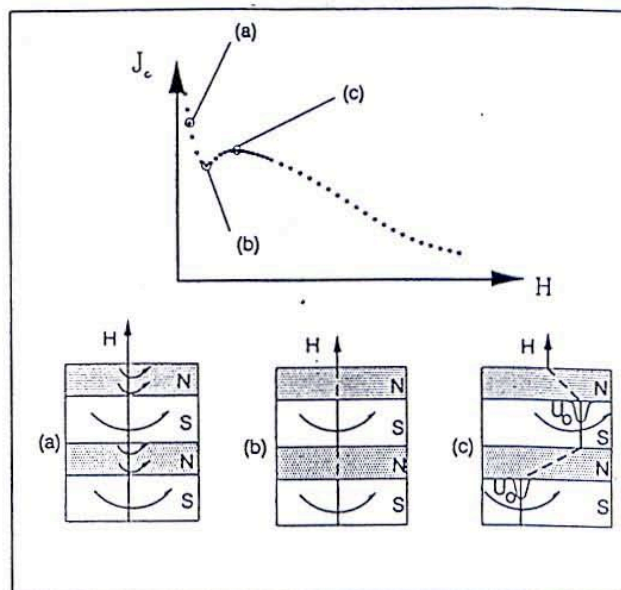
no longer present. Within this model it is difficult however to understand the role of the layering. The other plausible explanation is the magnetic decoupling mechanism proposed by Clem,[16] which is closely related to the behaviour of the flux line lattice in a superconducting transformer. The basic idea is illustrated in Fig. 9. At low fields (a) there is a rigid vortex lattice. As the field is increased, the intervortex distance decreases, producing a nearly homogeneous field distribution in the Ge layers (b). This effectively leads to a decoupling of the vortex lattice from layer to layer, leaving a system of stacked 2D pancake vortex lattices in each Pb layer. The vortices can rearrange themselves within each layer to take advantage of the available pinning centers (c), thus increasing the critical current. This is illustrated in Fig. 9 (c) showing schematically trapped vortices in pinning potential wells U_0.

CONCLUSIONS

We briefly reviewed some of the most important structural and superconducting properties of low T_c Pb/Ge and Al/Ge multilayers. Since the thickness and the composition of the layers can be well controlled, dimensional transitions and flux lattice structures can be studied in detail. The low T_c multilayers offer an ideal testing bed to study or compare the properties of naturally layered materials such as the high T_c materials.

REFERENCES

1) Schuller, I.K. in "Physics, Fabrication, and Applications of Multilayered Structures", Plenum Press, New York (1988)

2) For a recent review see for instance Schuller, I.K., Guimpel, J., and Bruynseraede, Y., "Artificially layered superconductors", Mater. Res. Bull., Vol. 25, 29 (1990)

3) Fullerton, E.E., Schuller, I.K., Vanderstraeten, H., and Bruynseraede, Y., "Structural refinement of superlattices from X-ray diffraction", Phys. Rev. B, Vol. 45, 9292 (1992)

4) Locquet, J.P., Neerinck, D., Vanderstraeten, H., Sevenhans, W., Van Haesendonck, C., Bruynseraede, Y., Homma, H., and Schuller, I.K., "Superconductivity in coupled Pb/Ge and Pb/C multilayers", Japan J. Appl. Phys., Vol. 26, 1431 (1987)

5) Neerinck, D., Temst, K., Vanderstraeten, H., Van Haesendonck C., Bruynseraede, Y., Gilabert, A., and Schuller, I.K., "Critical fields of weakly and strongly coupled superconducting multilayers", J. Phys.: Condens. Matter, Vol. 2, 6287 (1990)

6) Klemm, R.A., Luther, A., and Beasley, M.R., "Theory of the upper critical field in layered superconductors", Phys. Rev. B, Vol. 12, 877 (1975)

7) Takahashi, S. and Tachiki, M., "Theory of the upper critical field of superconducting superlattices", Phys. Rev. B, Vol. 33, 4620 (1986)

8) Koyama, T., Takezawa, N., Naruse, Y., and Tachiki, M., "New continuous model for intrinsic layered superconductors", Physica C, Vol. 194, 20 (1992)

9) Banerjee, I., Yang, Q.S., Falco, C.M., and Schuller, I.K., "Anisotropic critical fields in superconducting superlattices", Phys. Rev. B, Vol. 28, 5037 (1983)

10) Neerinck, D., Temst, K., Van Haesendonck, C., Bruynseraede, Y., Gilabert, A., and Schuller, I.K., "Dimensional transition in the fluctuation conductivity of Pb/Ge superconducting multilayers", Europhys. Lett., Vol. 15, 637 (1991)

11) For a review see Skocpol, W.J. and Tinkham, M., "Fluctuations near superconducting phase transitions", Rep. Prog. Phys., Vol. 38, 1049 (1975)

12) Takahashi, S. and Tachiki, M., "New phase diagram in superconducting superlattices", Phys. Rev. B, Vol. 34, 3162 (1986)

13) Clem, J.R., "Two-dimensional vortices in a stack of thin superconducting films: a model for high-temperature superconducting multilayers", Phys. Rev. B, Vol. 43, 7837 (1991)

14) Neerinck, D., Temst, K., Baert, M., Osquiguil, E., Van Haesendonck, C., Bruynseraede, Y., Gilabert, A., and Schuller, I.K., "Transition in the flux lattice of artificially layered superconductors", Phys. Rev. Lett., Vol. 67, 2577 (1991)

15) Fisher, D.S., Fisher, M.P.A., and Huse, D.A., "Thermal fluctuations, quenched disorder, phase transitions, and transport in type II superconductors", Phys. Rev. B, Vol. 43, 130 (1991)

16) Ekin, J.W. and Clem, J.R., "Magnetic coupling force of the superconducting dc transformer", Phys. Rev. B, Vol. 12, 1753 (1975)